Available online at www.sciencedirect.com
SCIENCE DIRECT®
Organic Geochemistry 35 (2004) 1461–1477
Organic Geochemistry
www.elsevier.com/locate/orggeochem

A new approach to interpreting Rock-Eval S_2 and TOC data for kerogen quality assessment

Birger Dahl [a,*], Jørgen Bojesen-Koefoed [b], Anders Holm [a], Holger Justwan [a], Egil Rasmussen [c], Erik Thomsen [b]

[a] Department of Earth Sciences, University of Bergen, Allégaten 41, 5007 Bergen, Norway
[b] Geological Survey of Denmark and Greenland (GEUS), Thoravej 8, DK 2400 Copenhagen, Denmark
[c] Pegis AS, Nils Langhellesvei 66, 5148 Bergen, Norway

Available online 15 September 2004

Abstract

A simple method for application in source potential mapping is used to assess the original oil and gas potentials in source rock horizons based upon Rock-Eval potential (S_2) and total organic carbon (TOC) values. The method assumes that kerogens consist of mixtures of end-members with assigned hydrogen index values. Based on suggested algorithms, the average amounts of oil-prone, gas-prone and inert organic material over source rock intervals are determined in TOC units. The method uses regression lines from plots of remaining hydrocarbon potentials (S_2) versus total organic carbon (TOC), and "quick-look" transparent overlays are used to read the appropriate kerogen mixture.

Mineral matrix effects during pyrolysis, when strong, can cause erroneous results. This effect which occurs for oil-prone kerogens and adsorptive minerals can cause problems particularly for lean samples (S_2 = 0–3 mg HC/g rock) whilst the errors for richer samples are less.

The method is applied on three sections of Upper Jurassic organic-rich rocks from the Danish North Sea sector, which are at different maturity stages. One of these sections is dominated by gas-prone material, one is dominated by oil-prone material and the third section contains a mixture of oil- and gas-prone material.

The method has been compared with other methods that split kerogens in oil and gas generating potential and has given reasonable results.

Experience using the method and a presented example suggest that sedimentological, system tract information may be derived from S_2 to TOC cross-plots. A constructed modelling example suggests that the end-member concept used in this approach may be used in forward type source rock prediction models when combined with sedimentological models. The resulting S_2–TOC plots can be used in order to check the forward modelling results against observed values.

1. Introduction

The organo-facies maps presented in the literature are usually qualitative with respect to oil and gas generation because only average total organic carbon (TOC), petroleum potential (S_2), or the dominant kerogen type are presented (e.g. Demaison and Moore, 1980; Cooper and Barnard, 1984; Isaksen and Ledje, 2001).

In order to assess the petroleum composition in the trap, petroleum potential maps should be divided into their proportions of oil and gas (primary) producing constituents as proposed by Dahl and Yukler (1991)

* Corresponding author.
E-mail address: birger.dahl@geo.uib.no (B. Dahl).

0146-6380/$ - see front matter © 2004 Elsevier Ltd. All rights reserved.
doi:10.1016/j.orggeochem.2004.07.003

and Dahl and Meisingset (1996). These constituents approximate what Cooles et al. (1986) described as labile and refractory kerogen constituents.

The relative amounts of oil- and gas-producing organic material can be determined by combined pyrolysis-gas chromatography (pyrolysis GC) of source rock samples during which the residual petroleum potential is resolved into gas and liquid components, i.e. the amount of C_{1-5} and C_{6+} (Pepper and Corvi, 1995) or C_{1-5}, C_{6-14} and C_{15+} (Horsfield, 1989). The magnitude of the hydrocarbon potential that yields gas (or oil) can thus be determined by multiplying the relative gas fraction magnitude determined from pyrolysis GC with the hydrocarbon potential, S_2.

Quantitative visual kerogen determinations can also be used to assess the approximate quantity of oil- and gas-producing components in the kerogen (Mukhopadhyay et al., 1985). The calculated fractions of gas versus the sum of oil and gas can be mapped and used to split the hydrocarbon potential map into gas and oil potential maps.

Rock-Eval pyrolysis and TOC determinations are the most widely used methods to characterise source rocks. Traditionally, the hydrogen index (HI) is used to assess the oil and gas potential of source rocks, unless calibrations between the hydrogen index and pyrolysis GC are done (Pepper and Corvi, 1995). Pepper and Corvi (1995) proposed to quantify and work with the active, petroleum generative carbon by multiplying the organic carbon with a factor that represents the carbon equivalent of the potential hydrocarbon yield. This active carbon is divided into oil generating and gas generating parts using the *G* factor derived from pyrolysis GC. When no pyrolysis GC data exist, they apply a global correlation between the restored HI and the gas fraction (*G*, in this paper referred to as *G*0) of the active carbon. The global calibrated *G*0 trend has a dynamic range from about 0.18 for HI = 1000 to approximately 0.6 for HI = 0 mg HC/g org.C. This means that the *G*0 factor cannot give less oil potential than about 40% of the total potential.

Barnard et al. (1981) suggested a method that de-convoluted and quantified the kerogen composition of samples using Rock-Eval data combined with vitrinite reflectance and spore coloration. This method was used by Cooper and Barnard (1984) to map the Upper Jurassic source rocks of the North Sea with respect to their dominant kerogen constituents.

Due to the ease of the Rock-Eval method relative to pyrolysis GC analysis and visual kerogen typing, most geochemical databases contain more Rock-Eval data compared to pyrolysis GC and quantitative petrographic kerogen typing. Division of source rock hydrocarbon potential into oil and gas producing capabilities can therefore be difficult to perform.

This paper suggests a practical exploration tool that uses Rock-Eval and TOC data to give a rapid assessment of the average oil- and gas-producing constituents in source rocks. The method also determines the average amount of inert organic carbon in the section and assumes that the pyrolysable part of the kerogen can be subdivided in two ideal kerogen end-members with fixed initial hydrogen indices. The method cannot replace pyrolysis GC and visual kerogen data for assessing oil and gas potentials, but rather enables the petroleum geochemist to fill in gaps where pyrolysis GC and visual kerogen data are few.

2. Method description

2.1. Principles

The method described is not intended to estimate gas or oil potential of individual samples, but rather an average value for a source rock section or a sample suite. Consequently, all Rock-Eval values are average or mean values for the appropriate source rock sections.

The method presented is based on cross-plots of S_2 versus TOC as described by Clayton and Ryder (1984) and Langford and Blanc-Valleron (1990), and regards the TOC to be a linear function of S_2 with the HI as the slope of the curve. (It should be noted that parameters derived from the method are average values and not individual analytical values or ratios of such.) The HI derived from the regression line in such cross-plots measures the average HI of the organic material. The intersection of the regression line with the TOC axis is a measure of the average, inert organic carbon in the sample population (Cornford, 1994; Cornford et al., 1998). In our view, kerogen consists of oil-prone and gas-prone kerogen components that can be assigned fixed HI values, and the relative proportions of these constituents can be derived from the average HI found by the regression line. These kerogen constituents with associated HI values are referred to as kerogen end-members (see discussion below). Our method quantifies the average inert organic carbon plus the two oil- and gas-prone end-members in % wt or TOC units. The average hydrocarbon potential with respect to the two constituents can be deduced using the hydrogen index definition described below.

2.2. Determination of the inert component

The regression line through most S_2–TOC populations

$$y = ax + b \tag{1}$$

is equivalent to

$$\mathrm{TOC} = aS_2 + b. \quad (2)$$

Should the regression line pass through the origin, $b = 0$. With few exceptions (using S_2 vs TOC), the authors find that the line intersects the positive TOC axis. Langford and Blanc-Valleron (1990) observed regression lines offset from the origin, but believed this was caused by matrix effects associated with the pyrolysis (described by Espitalié et al., 1980; Katz, 1983).

Sedimentary organic matter will usually have a fraction of inert organic material, which does not fragment during pyrolysis, and we agree with Cornford (1994) that it leads to a regression line that is offset from the origin. This offset may consequently result from a combination of indigenous inert organic carbon and matrix retention effects during pyrolysis. It is, however, possible to quantify and adjust the effect of the matrix-induced component (see discussion on matrix effects below).

The intersection b represents the average amount of inert or "dead organic carbon", in the analysed section.

The slope of the curve

$$a = \mathrm{TOC}/S_2 = 100/\mathrm{HI} \quad (3)$$

since the hydrogen index (HI) is defined HI = 100 S_2/TOC.

The hydrogen indices derived from TOC versus S_2 plots represent therefore an average or mean "live organic material" of the analysed section. ("Live" organic material means the proportion of the organic material that is pyrolysable.) When the regression line is not intersecting at the origin, this hydrogen index is *different* from the arithmetic mean of the HI calculated from the same sample set. In cases were $b = 0$ and the regression line intersects the origin, the hydrogen indices derived from arithmetic mean and the slope of the curve should be the same. In practice, their values are similar, but not identical. The average HI of the "live organic material" from a source rock section can alternatively be calculated when the inert organic component, hereafter referred to as TOC(inert), is subtracted from the overall total organic carbon, referred to as TOC(observed):

$$\mathrm{HI(live)} = 100S_2/(\mathrm{TOC(observed)} - \mathrm{TOC(inert)}). \quad (4)$$

Since both TOC(observed) and TOC(inert) always have positive values and TOC(observed) > TOC(inert), the HI(live) will always be larger than the arithmetic mean, HI(mean). This implies that the source rock sections (or samples) containing inert organic material have an apparent hydrogen index which is lower than the real HI of the sections (or samples) represented by the HI(live). In principle, the analysed sections (or samples) containing inert organic carbon will consequently have a better source rock quality than suggested by the Rock-Eval analysis.

As demonstrated above, there are two different ways to obtain the HI(live): either from the slope of the regression curve or from Eq. (4). Since each method is based on slightly different approaches, the same values for HI(live) should not be expected. Close values will, however, indicate that the method gives reasonable results.

2.3. Composition of the active kerogen

If the HI of the average "live" kerogen is assumed to consist of oil-prone (sapropelic) and gas-prone (vitrinitic) material (referred to as two ideal end-members, see discussion below) with associated hydrogen indices HI(oil) and HI(gas), then the fraction of each component, m and n, respectively, can be de-convoluted according to

$$\mathrm{HI(live)} = \mathrm{HI(oil)}m + \mathrm{HI(gas)}n \quad (5)$$

and, due to mass balance,

$$m + n = 1. \quad (6)$$

The hydrogen index parameter changes, however, with increasing kerogen transformation (TR) as defined by Espitalié and Bordenave (1993). Eq. (5) can thus be changed to

$$\mathrm{HI} = \mathrm{HI(oil)}(1 - \mathrm{TR})m + \mathrm{HI(gas)}(1 - \mathrm{TR})n \quad (7)$$

that takes into account the change of the source rock quality as a function of hydrocarbon generation. It should be noted that the hydrogen index does not vary linearly with transformation ratio (TR) as shown by Espitalié et al. (1987) and Justwan and Dahl (2005). However, a linear relationship can be assumed because the deviation from linearity is small. Linear correlation coefficients (R^2) through TR–HI curves are approximately 0.99, using the relationships between TR, HI and α (see definition below) given by Justwan and Dahl (2005).

If differential degradation of the various kerogen end members should be taken into account, Eq. (7) can be changed to HI = HI(oil) (1 − TR(oil))m + HI(gas) (1 − TR(gas))n where TR(oil), and TR(gas) are the transformation ratios for oil- and gas-prone kerogens, respectively.

In order to split the average TOC into oil-prone and gas-prone organic carbon, GORP (gas-oil-ratio-potential) is defined (Eq. (8)) and multiplied with the "live" TOC (Eq. (9))

$$\mathrm{GORP} = m/(m + n), \quad (8)$$

$$\mathrm{TOC(live)} = \mathrm{TOC(observed)} - \mathrm{TOC(inert)}. \quad (9)$$

The dominant oil producing and gas producing TOC constituents, TOC(oil) and TOC(gas), respectively, are calculated according to

$$\mathrm{TOC(oil)} = \mathrm{TOC(live)}(1 - \mathrm{GORP}), \quad (10)$$

$$\mathrm{TOC(gas)} = \mathrm{TOC(live)GORP}. \quad (11)$$

2.4. Petroleum potential restoration

If the kerogen of the analysed horizon has been subjected to thermal degradation, the average residual hydrocarbon potential must be restored to its original potential.

To enable the restoration of the original hydrocarbon potential, the transformation ratio of the total kerogen (or kerogen components) at different depths of burial have to be determined. Transformation ratios can be found empirically by regional geochemical studies (e.g., Espitalié et al., 1987; Dahl and Augustson, 1993) or from basin simulation runs using software with a kinetic subroutine.

The method to find the original TOC proceeds via determination of organic material lost from natural hydrocarbon generation. This amount is subsequently added to the observed or measured amount in order to obtain the restored S_2 and TOC

$$S_2(\mathrm{lost}) = S_2(\mathrm{restored}) - S_2(\mathrm{observed}), \quad (12)$$

where

$$S_2(\mathrm{restored}) = S_2(\mathrm{observed})/(1 - \mathrm{TR}). \quad (13)$$

To restore the TOC a simple principle stoichiometric relationship is used

$$\mathrm{kerogen} \rightarrow \mathrm{petroleum} + C(\mathrm{residue}).$$

Depending on the bulk composition (i.e. the carbon versus hydrogen and other elemental content) of the petroleum, a constant α (see discussion below) can be derived in order to convert S_2(lost) to TOC(lost)

$$\mathrm{TOC(lost)} = S_2(\mathrm{lost})\alpha. \quad (14)$$

TOC(lost) is subsequently added to TOC(observed) to obtain TOC(restored).

The restoration of TOC can be done using the formula that follows this principle:

$$\mathrm{TOC(restored)} = \mathrm{TOC(observed)} + [S_2(\mathrm{observed})\mathrm{TR}/(1 - \mathrm{TR})]\alpha. \quad (15)$$

Based on this reconstruction, a new, restored, "live" hydrogen index value can be calculated for use in Eq. (6) in order to find the relative proportions of oil- and gas-prone kerogens

$$\mathrm{HI(live, restored)} = 100 * S_2(\mathrm{restored})/(\mathrm{TOC(restored)} - \mathrm{TOC(inert)}). \quad (16)$$

The three TOC components can now be obtained by using Eqs. (9)–(11) where TOC(restored) replaces TOC(observed) in Eq. (9).

The principal steps of the method are illustrated in the flow chart shown in Fig. 1 and explained through practical use below.

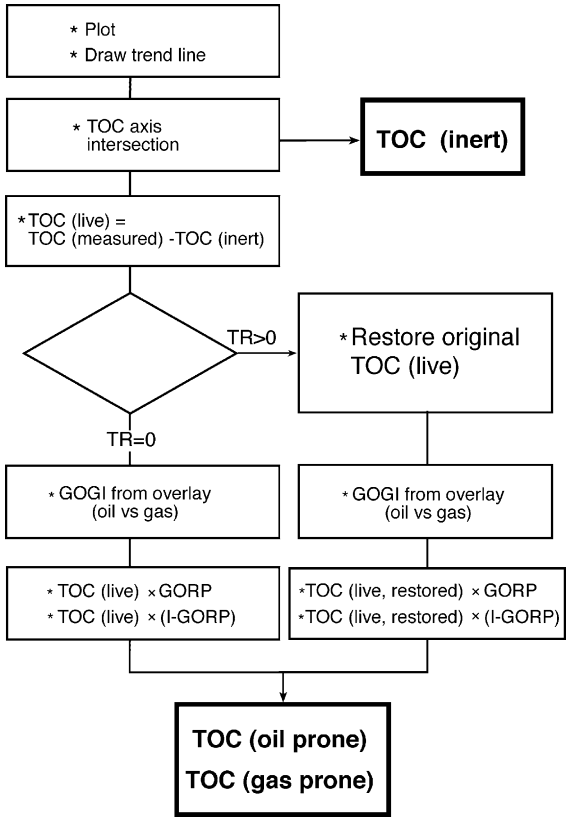

Fig. 1. Schematic procedure for execution of the method.

3. Some of the parameters used in the method: a brief discussion

3.1. The stoichiometric factor α

This parameter is derived from the assumed gross elemental composition of the petroleum products formed from an ideal kerogen. It is used as a constant in this context, but will obviously change as the kerogen matures. It is deduced from the following simple relationship:

$$\alpha = 0.1C/(C + gH), \quad (17)$$

where C and H are the atomic weights of carbon and hydrogen, whilst g is the number of H-atoms. A S_2 gross composition CH_2, as suggested above, gives $\alpha = 0.086$, which indicates that 86%wt of the petroleum is carbon. Espitalié et al.'s (1987) method estimates 83%wt carbon in the petroleum or pyrolysate equivalent, whilst the group at Lawrence Livermore National Laboratory, California, uses 85%wt (A. Burnham, pers. commun.).

Since the most hydrogen-rich petroleum that can be obtained is methane (CH_4), one extreme value for α is 0.075. The other extreme is obtained by letting the hydrogen amount in Eq. (17) approach zero. This results

in α approaching 0.1. Consequently, α is between 0.075 and 0.1.

Eq. (17) is, however, a simple relationship and does not take into account the amounts of atomic nitrogen, sulphur and oxygen that are produced. The accuracy of α may be improved by taking these factors into account

$$\alpha = 0.1\mathrm{C}/(\mathrm{C} + \mathrm{pH} + q\mathrm{N} + r\mathrm{S} + s\mathrm{O}), \quad (18)$$

where q, r and s are the relative numbers of nitrogen, sulphur and oxygen atoms, respectively.

Using a gross S_2 composition C H_2 $N_{0.001}$ $S_{0.003}$ $O_{0.0045}$ suggested by Tissot and Welte (1978) as average values for oils, gives $\alpha = 0.084$.

The extreme values obtained by letting the number of hydrogen atoms, p, go towards 4 and 0 now give $\alpha = 0.074$ and 0.098, respectively. These values are, not surprisingly, different from the values obtained by using carbon and hydrogen only and show that only H/C ratios may apply well as an approximation (Baskin, 1997).

3.2. Source rocks, organic facies and kerogen end-members

The subdivision of sedimentary organic matter into kerogen types is in principle an end-member concept. Kerogens and organic matter in sediments are, however, generally regarded as heterogeneous substances. The concept of using ideal end-members with assigned hydrogen indices, or even with assigned kinetic parameters for kerogen breakdown, as suggested by Pepper and Corvi (1995), is consequently debatable (e.g Tyson, 1995, pp. 367–382). Pepper and Corvie suggested that all source rocks in the world would break down according to the kinetic scheme of one of five kerogen end-members.

Baskin (1997) suggested that the general H/C ratio of the organic matter in a source rock can be determined by averaging the relative quantities plus the ideal H/C ratios of the marcerals present. The method is based on the concept that H/C ratios can be determined from microscopic observations (Jones and Edison, 1978) by relating them to a standard van Krevelen diagram.

Jones (1987) defined seven types of organic facies, characterised primarily by marceral composition, H/C and O/C ratios and Rock-Eval pyrolysis results at $R_0 \sim 0.5\%$. The organic facies types, named A, AB, B through to D were assigned to typical depositional settings and suggested primary products (oils and natural gases). These facies are composed of mixtures of algal/bacterial hydrogen-rich material (Organic Facies A) through to vitrinite (Organic Facies C) and inertinite/oxidised organic matter (Organic Facies D). The compositions of these facies types are not only dependant on the original input material, but also on the availability of oxygen during and after deposition. Jones (1987) suggests that oxic environments convert hydrogen-rich organic matter into organic matter with lower H/C (i.e., the organic matter is transformed from Organic Facies B to that of Facies D).

These organic facies types cannot strictly be called end-members, but are rather typical, or common, kerogen compositions for different geological settings derived from the deposition and preservation of organic matter. It seems, however, to be the suggestion in the literature that is closest to the end-member kerogen system proposed in the presented method.

The method in this paper requires that source rocks in general be regarded as composed of three kerogen end-members where two of them (those that produce oil or gas) can be calibrated according to a general understanding of the source rock system and its geological setting. In view of the complex composition of OM in sedimentary rocks, this concept can only be a simplification of real systems.

In the method presented, organic matter in a source rock is regarded as composed of a mixture of three kerogen end-members with similar features to those of Jones (1987) Organic Facies (i.e., purified versions of Organic Facies B, C and D, see discussion Ch 4.1).

Organic matter in source rocks is heterogeneous in character, and it is obvious that the proposed method needs to be used with caution. It is recommended therefore to acquire a fairly good knowledge of the source rock system and its palaeo-environment of deposition prior to using this method. During this process, it will be necessary to assess the various end-members based upon a combination of organic petrography, Rock-Eval pyrolysis, combined pyrolysis and gas-chromatography results and, if available, elemental compositions.

Sapropelic or oil-prone material seems to have the largest variation (Hunt, 1996, p. 333) and it is believed that large fluctuations in terrestrially derived waxy components can cause problems for the method. A second oil-prone component would be welcome in the method to handle this waxy component. This will, however, require the solution of three unknowns from two equations, which is not possible.

Applications of the method in geological settings associated with large and rapid shifts in bottom water oxygen contents and shifts in depositional rates of clastic material, such that the chemical composition of the same organic matter type changes considerably, can also be problematic. Jones (1987) refers to the grading of reworked Organic Facies B into Organic Facies D under influence of an oxygenated water column during deposition of the Upper Jurassic of the Jeanne d'Arc Basin, offshore eastern Canada. It is also obvious that differences in AB and B are partly due to the oxic–anoxic situation during and right after deposition of the material. In settings where the "end-member material" can change considerably, chemically defined end-members will be

difficult to apply and will have no meaning. It is believed that samples from such sections will signal a fairly chaotic S_2 versus TOC plot and give no apparent trends.

On the other hand, chaotic plots can also occur due to rapid vertical shifts in the kerogen blends (e.g., when shelf-derived gravity flows containing large amounts of vitrinite and inertinite are interbedded with Organic Facies AB or B, this may cause confusing S_2 versus TOC plots to appear).

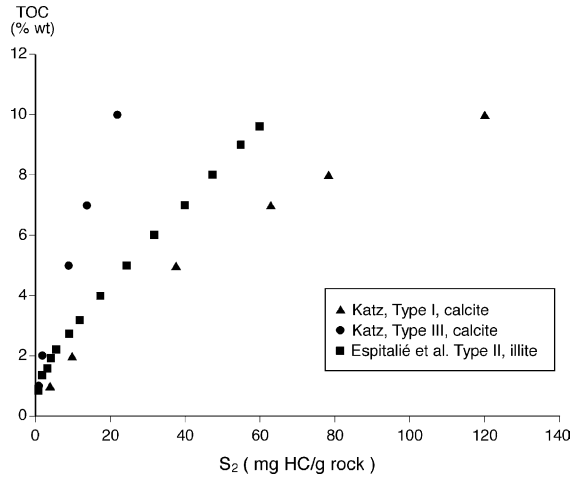

Fig. 2. Plot of S_2 and TOC results performed on various mixtures of kerogens and minerals to show the linear deviation that can occur in Rock-Eval pyrolysis experiments. The data are from Espitalié et al., 1980 and Katz, 1983.

3.3. Matrix effect and uncertainties in Rock-Eval pyrolysis results

Various authors (Peters, 1986; Katz, 1983; Espitalié et al., 1980) have shown that mineral matrix can reduce the S_2 pyrolysis yield, resulting in a reduction of the hydrogen index and lower apparent source quality. The suggested mechanism for this effect is the adsorption of heavy pyrolysate components onto clay minerals where they are converted to non-volatile char and light material thus reducing the S_2 and HI. These studies were based on isolated kerogens diluted with various minerals. In general, it seems that organic-rich samples with low production of heavy liquid hydrocarbons combined with a low adsorbing matrix give the least error in S_2 values. S_2–TOC plots of selected data sets (Fig. 2) from Espitalié et al. (1980) and Katz (1983) show decreasing linearity with increasing matrix effects. Fig. 2 shows that Type III kerogens in calcite are linear whilst Type I in calcite are non-linear. This plot shows that the presented method will give erroneous results for the most adsorptive matrix–kerogen combinations.

In order to illustrate how large matrix errors can be, a generalised S_2 vs TOC plot of Espitalié et al.'s (1980), Type II kerogen in illite, is made (Fig. 3) together with the ideal linear trend, HI = 620 mg HC/g org.C. This mineral–kerogen combination gave largest adsorption effects (Espitalié et al., 1980) and may be regarded as a "worst case" example. The resulting plot can be subdivided into three sections that are close to linear. The trend for the lowest values (A, S_2 = 0–3 mg HC/g rock)

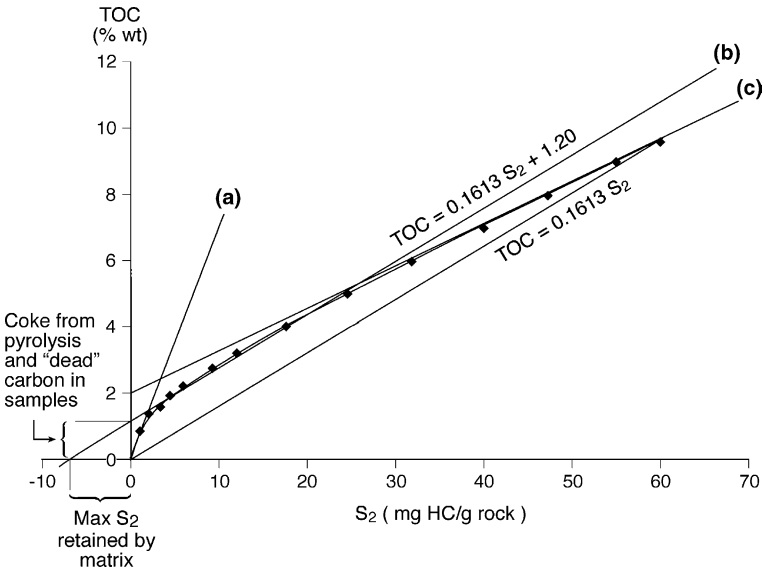

Fig. 3. Profile in a S_2–TOC plot showing the errors occurring during Rock-Eval pyrolysis as the result of pyrolysate retained by the mineral matrix. Data are from Espitalié et al., 1980. S_2 suppression values and correction factors referred to in the text can be inferred from this curve.

is most deviated and gives lower HI (212mg HC/g org.C) relative to the ideal trend. The middle values (B, S_2 = 3–25 mg HC/g rock) are parallel with the ideal trend (same HI) and the highest values (C, S_2 = 25–60 mg HC/g rock) give slightly too high HI (775 mg HC/g org.C).

The error is largest for the lowermost S_2 range (0–3) and S_2 = 3 mg HC/g org.C could be suppressed with 5 mg HC/g org.C. A correction factor for S_2 of 2.9 could be applied within this S_2 range. Application of the presented method on the lowermost S_2 range (trend A) will give dominantly gas-prone kerogen, and it will be useless in such kerogen–matrix combinations unless the S_2 values are corrected for the S_2 suppression.

For the middle range (B) where the trend parallels the ideal HI, the kerogen splitting will be correct. This line intersects the TOC axis at 1.2%wt and the negative part of the S_2 axis at −7.4 mg HC/g rock. It is suggested that the negative intersection with the S_2 axis indicates the average magnitude of material that is retained and the corresponding residue formed due to the matrix retention effect, and this negative value can be used to correct for this effect. If a low hydrogen containing elemental composition (e.g. C_5H with $\alpha = 0.098$) is anticipated for the retained material, then the TOC content is 0.73%wt. This is 0.47%wt lower than indicated by the TOC-axis intersection and may indicate that the kerogen used to set up this profile contained minor amounts of inert carbon.

The upper range needs a correction factor for S_2 = 1.3, progressively approaching 1.0 beyond 60 mg HC/g rock, and the TOC axis intersection must be subtracted by 1.9%wt TOC in order to find the TOC (inert). Ranges over S_2 = 60 mg HC/g rock will approach the ideal trend, and corrections will not be needed.

It is beneficial to have control on the mineral matrix composition which can be obtained by XRD analysis of the rocks. How aggressive these minerals are with respect to hydrocarbon adsorption can be examined by conducting experiments such as Espitalié et al. (1980) and Katz (1983). The Rock-Eval analysis and the presented method are both quite rough, and for practical purposes the method should be applied without corrections as soon as S_2 values are above 3–4 mg HC/g rock. Corrections without knowledge of the adsorptive effects, determining best case–worst case values can also be applied. When the S_2 range is 3–25 mg HC/g rock (case B, Fig. 3) in absorptive matrices, and the TOC (inert) is not corrected for the absorptive effect, the average source rock potential for the analysed section will be reduced by 3–9 mg HC/g rock using HI end-members 250 and 700 mg HC/g org.C, if Fig. 3 is used as a "worst" case.

4. Practical application

The most difficult part during the application of the method is to find the regression line through the analysed data set in order to determine HI(live) and TOC-(inert). When the regression line slope and the intersection with the TOC axis are determined, the remaining aspects represent fairly simple calculations using the algorithms suggested above. If the rock sequence has yielded hydrocarbons, the calculations are cumbersome since the transformation status of the source rock horizon needs to be taken into account. In order to get around the problem of determining the regression line and to ease the calculations, a set of transparent overlays, which can be applied to plots, is suggested. S_2 and TOC values must be plotted on a graph upon which the trend-lines are drawn through the various S_2–TOC populations. The overlays are superimposed on the trend line and the kerogen mixture (m and n in Eqs. (5) and (6)) is read from the overlay.

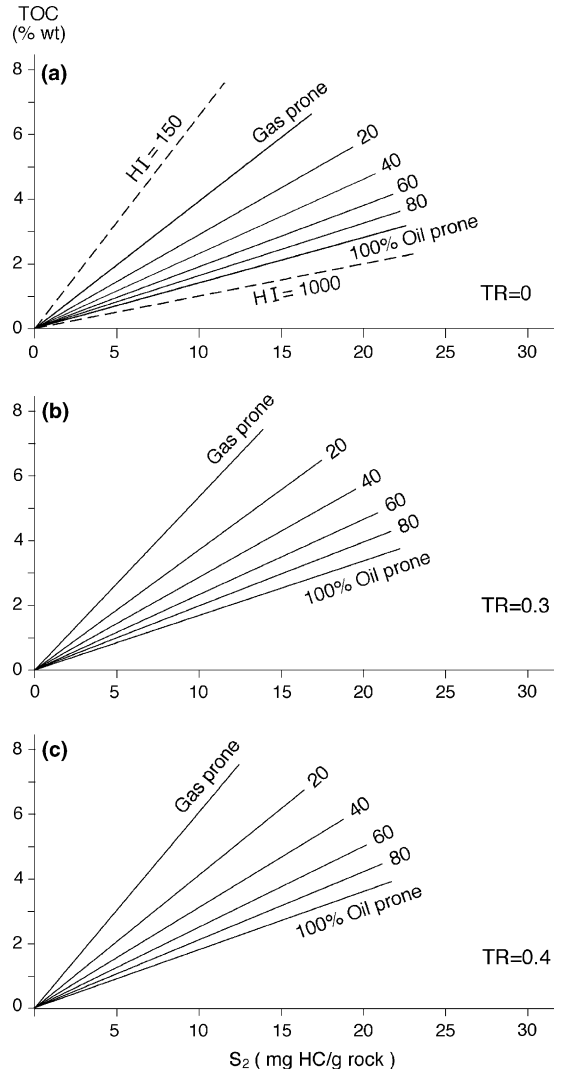

Fig. 4. Selected overlays constructed for transformation ratios (TRs) 0.0, 0.3 and 0.4.

Because the S_2 and TOC-values change with increasing maturity, overlays for different stages of kerogen transition have to be prepared. By inserting the ideal end-member values together with TR value(s) into Eqs. (5)–(7) together with fractions (m and n) of oil- and gas-prone kerogen, the hydrogen indices for various mixtures of these end-members can be calculated. The overlays can be made by converting these resulting hydrogen indices to lines in S_2 versus TOC plots.

To be able to use such overlays, it is necessary to plot the data in a standard format axis system where S_2 is the x-axis and TOC is the y-axis. Examples of overlays are shown in Fig. 4 for the cases when the transformation ratios are 0.0, 0.3 and 0.4. The overlay shows that spacing between the various mixtures with 20% increments are non-linear, with the poorest resolutions in the area with high proportions of oil-prone kerogens. It also shows that the sectors and the slope angle increase with increasing kerogen transformation.

The method is outlined schematically in Fig. 1. The upper box in Fig. 1 "Plot and draw trend line" is demonstrated in diagram (a) of Fig. 5. The trend line intersection with the TOC axis gives the average inert organic carbon, TOC(inert), as suggested by the next two boxes in Fig. 1.

TOC(live) which subsequently is split into TOC(oil) and TOC(gas) is found from Eq. (9). The working process shown in Fig. 1 indicates that the path to follow is dependent on the generation situation of the analysed section. If the section is immature and $Tr = 0$ (Fig. 1), then the transparent overlay prepared for $Tr = 0$, shown in Fig. 4(a), is superimposed on the plot. It is applied such that its TOC axis falls upon the TOC axis of the plot, and its origin is located at the trend line intersection with the TOC axis, shown in Fig. 5(b). The GORP factor can now be read from the overlay and used to obtain TOC(oil) and TOC(gas) (Eqs. (10) and (11)).

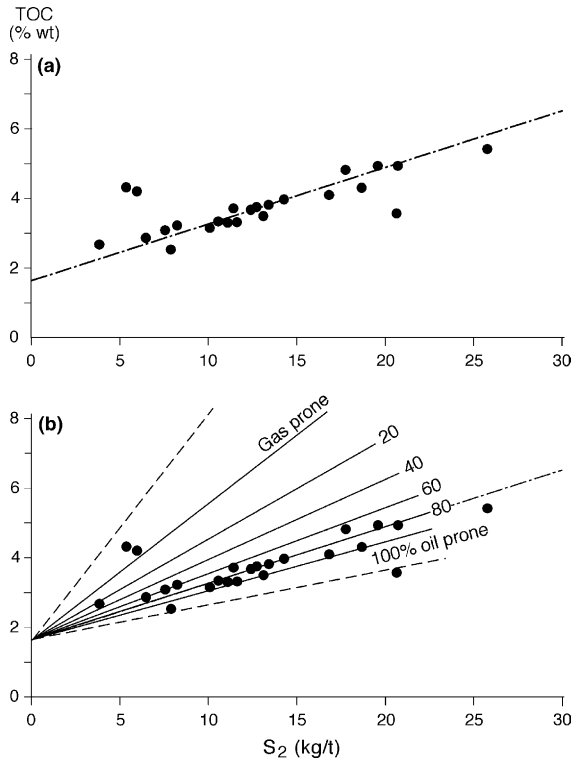

Fig. 5. Method application on the immature Upper Jurassic "Hot Unit" of Well Bo-1. (a) Plot of S_2 and TOC data (Table 1) in standard plot axis format. (b) Overlay superimposed on plot to read the kerogen mixture (m and n). The highest TOC–S_2 pair is not shown in the plot, but falls on the trend line.

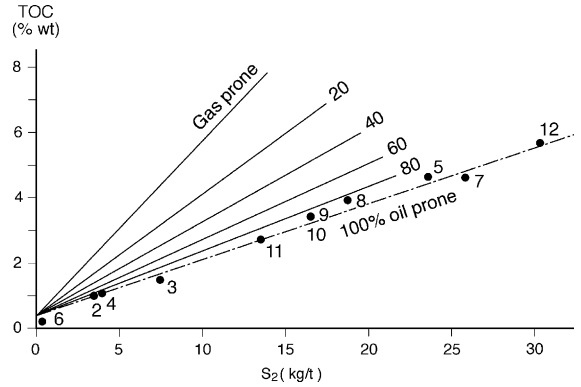

Fig. 6. Method application on a cored section of the Upper Jurassic "Hot Unit" of Well Jeppe-1. (a) Plot of S_2 and TOC data (Table 1) in standard plot axis format. (b) Overlay superimposed on plot to read the kerogen mixture (m and n).

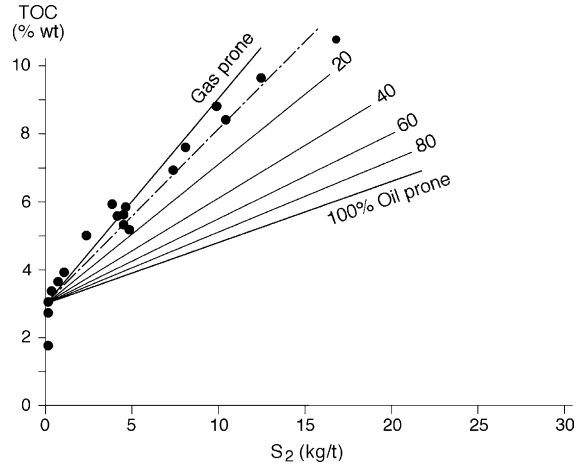

Fig. 7. Method application on the sequence Volg-20 (Andsbjerg and Dybkjaer, 2003) of Volgian age of Well Jeppe-1. (a) Plot of S_2 and TOC data (Table 1) in standard plot axis format. (b) Overlay superimposed on plot to read the kerogen mixture (m and n).

If the analysed section has yielded hydrocarbons ($Tr > 0$, Fig. 1), then the TOC(live) must be restored back to its original value (TOC before the hydrocarbon generation started) by first using Eq. (16) and secondly Eq. (9) to obtain TOC(live, restored). (Alternatively, replace TOC(observed) with TOC(live) in Eq. (15).) Select the overlay for the appropriate transformation situation. Overlays for Tr values 0.3 and 0.4 (Figs. 4(d) and (e)) are used to obtain the GORP factor for the two analysed sections from Jeppe-1 shown in Figs. 6 and 7. This factor is used to obtain the TOC(oil) and TOC(gas) by multiplication with the TOC (live, restored).

4.1. Examples

The three examples used to demonstrate the method are from the Upper Jurassic source rock sections of the Farsund Fm in the Danish Central Graben. These organic-rich shales in the Graben Centre are deposited dominantly under anoxic conditions and are composed of fluorescing sapropelic material with minor amounts of vitrinite and inertinite, whilst the flanks and the platform areas contain increasing amounts of less-hydrogen-rich material as the distance to the paleo shore decreases. (e.g., Thomas et al., 1985). The dominating organic facies seem to be B with AB occasionally present in the deepest and northernmost parts of the Central Graben. The flanks and platform area are dominated by Organic Facies C and D, respectively (Cooper and Barnard, 1984; Jones, 1987).

In the examples considered, ''modified versions'' of Organic Facies B, C and D (Jones, 1987) are suggested as end-members (see discussion above). For Organic Facies B the vitrinite and possible inertinite components are hypothetically ''removed'' to obtain the oil-prone end-member HI(oil). This end-member will consequently have a hydrogen index in the upper range for Organic Facies B, around 700 mg HC/g org.C. For the gas-prone end-member, the hydrogen index from the upper range of Organic Facies C, 250 mg HC/g org.C. is suggested. Facies C contains subordinate amounts of herbaceous material, and includes a liquid component. The inert or ''dead carbon'' end-member, Facies D, consists entirely of inertinite with no generating potential (i.e., the HI = 0 mg HC/g org.C). These values are also in line with the values Cooper and Barnard (1984) used in their organic facies mapping of the Upper Jurassic, North Sea.

The clay minerals in the Upper Jurassic Farsund Formation in this area are generally dominated by illite (60–80%) with low smectite contents. The swelling and, consequently, the adsorptive properties of this illite are low (e.g., compared to the Mexican Gulf). In the upper part of the formation, kaolinite may dominate (H. Lindgreen, pers. commun.). XRD analysis on occasional samples shows also that organic-rich samples may be totally dominated by calcite.

The first example (Fig. 5 and Table 1) is from the Danish Well, Bo-1, which is located in the southern part of the Tail End Graben of the Danish Central Trough (Damtoft et al., 1992). The analysed section (2576–2710 m) comprises the immature ''Hot Unit'' of the Upper Jurassic Farsund Formation. It is a fairly rich section with TOC and S_2 values from 2.5%wt and 3.9 mg HC/g rock up to 8%wt and 36 mg HC/g rock, respectively. Generally good hydrogen index values, between 300 and 500 mg HC /g org.C, suggest the section to be dominated by oil-prone material, but with some minor gas-prone vitrinitic material. The plot in Fig. 5(a) shows a good trend. Three samples (2603 m, representing the highest HI value in the data set, and 2688 and 2697 m, representing low HI values) are outliers from the trend. The method suggests, not surprisingly, that the oil potential dominates the sequence (Table 2). The ratio between gas and oil, GORP is low (0.2), but the relative proportion of inertinitic TOC (Fig. 3(a)) is high and represents 34% of the TOC(total). The oil and gas potentials are 11 and 2.8 mg HC/g rock, respectively.

Quantitative attempts have not been made to assess errors due to the effect of matrix retention (see discussion above). The S_2 values in this plot (Fig. 5(a)) are, however, within the range suggested to give regression lines parallel to the trend line of the pure, unaffected end-member (Fig. 3). The regression line (Fig. 5(a)) intersects the negative S_2 axis at approximately 10.5 mg HC/g org.C (not shown). This is higher than 7.4mg HC/g org.C suggested by the experiments of Espitalié et al. (1980) and Fig 3. With a molecular composition for the retained heavy liquid of C_5H ($\alpha = 0.098$), an average carbon residue has been formed during pyrolysis equivalent to TOC = 1.0 or 0.8%wt, respectively. Using 0.8%wt to correct for the matrix effect reduces the TOC(inert) propotion from 34 to 17 %wt and increases the oil and gas generating part to 66 and 17%wt, respectively. Due to an expected moderately adsorbing mineral matrix this correction is probably too large such that the real situation is somewhere between the corrected and the uncorrected values.

The cored interval (4405–4419 m) in the Jeppe-1 ''Hot Unit'' produces a linear trend in the TOC versus S_2 plot (Fig. 6). Most of the samples have good source rock potentials and hydrogen index values around 500 mg HC/g org.C. The overlay (Fig. 4(b)) suggests a section which is completely dominated by oil-prone material. The inertinitic component is very low (TOC(inert) = 0.4%wt) and the gas potential is zero. The extrapolation of the regression line intersects the negative S_2 axis at −2.5 mg HC/g org C which is considerably lower than −7.4 mg HC/g org.C indicated in Fig. 3. This suggests that the matrix retention in this section may be quite low. An adjustment equivalent to the one

Table 1
Pyrolysis and TOC results from Upper Jurassic source rock sections of the Danish Central Trough Wells, Bo-1 and Jeppe-1

Depth (m)	S_1 (mg HC/g rock)	S_2 (mg HC/g rock)	HI (mg HC/g org.C)	TOC (%wt)	PI	T_{max} (°C)
Bo-1, pyrolysis results from the Upper Jurassic, Hot Unit						
2576	1.0	6.5	228	2.85	0.14	427
2579	1.7	18.7	438	4.27	0.08	424
2582	1.8	17.9	374	4.80	0.09	422
2585	1.0	11.5	307	3.75	0.08	423
2588	1.8	25.9	480	5.40	0.07	423
2591	1.1	19.6	402	4.89	0.05	419
2594	1.3	13.5	352	3.84	0.09	423
2597	1.0	13.1	373	3.50	0.07	421
2600	0.9	11.6	350	3.31	0.07	424
2603	1.0	20.7	586	3.53	0.05	418
2606	1.9	36.2	451	8.04	0.05	416
2609	0.9	14.4	363	3.97	0.06	424
2615	0.8	17.0	416	4.08	0.05	429
2624	1.1	20.7	421	4.92	0.05	427
2633	0.9	12.7	340	3.74	0.06	428
2643	0.5	7.4	291	2.53	0.06	430
2652	1.0	12.4	338	3.67	0.07	426
2661	0.8	10.1	321	3.13	0.08	430
2670	0.8	10.6	316	3.36	0.07	430
2679	0.6	11.1	338	3.28	0.05	430
2682	0.4	7.3	236	3.09	0.05	432
2688	0.8	7.0	166	4.19	0.11	429
2697	1.0	6.4	149	4.28	0.13	427
2707	0.4	3.9	145	2.70	0.09	433
2710	0.4	8.3	256	3.23	0.04	434
Jeppe-1, cored section from the Upper Jurasssic, Hot Unit						
4405	7.7	40.5	595	6.80	0.16	441
4407	3.4	16.7	491	3.40	0.17	441
4408	0.9	7.3	486	1.50	0.11	441
4409	1.7	4.0	363	1.10	0.30	440
4411	2.6	23.7	516	4.60	0.10	442
4411	0.2	0.4	180	0.20	0.38	442
4412	3.2	26.0	565	4.60	0.11	441
4414	3.3	18.9	485	3.90	0.15	443
4415	1.7	3.5	350	1.00	0.32	441
4417	2.7	16.6	488	3.40	0.14	441
4418	2.8	13.6	503	2.70	0.17	440
4419	5.0	30.5	500	6.10	0.14	442
Jeppe-1, pyrolysis results from the Volg-20 sequence						
4865	5.5	7.5	109	6.85	0.42	439
4867	3.1	4.2	75	5.59	0.42	435
4870	5.3	8.3	110	7.56	0.39	440
4872	9.4	17.1	159	10.70	0.35	439
4875	6.8	10.1	116	8.73	0.40	437
4877	8.0	12.7	133	9.55	0.39	437
4880	6.9	10.6	127	8.39	0.39	438
4882	3.1	4.5	81	5.57	0.41	438
4885	3.0	4.8	94	5.13	0.38	438
4887	3.0	4.6	86	5.33	0.40	439
4890	2.9	3.9	66	5.91	0.43	438
4892	3.2	4.6	80	5.79	0.41	438
4895	0.4	0.3	9	2.74	0.63	439
4897	0.4	0.3	11	2.66	0.57	438
4900	1.7	2.4	48	4.98	0.41	439
4902	0.5	0.5	16	2.89	0.54	439

Table 1 (*continued*)

Depth (m)	S_1 (mg HC/g rock)	S_2 (mg HC/g rock)	HI (mg HC/g org.C)	TOC (%wt)	PI	T_{max} (°C)
4905	0.3	0.1	5	1.82	0.75	431
4907	0.7	0.6	19	3.32	0.54	441
4910	0.8	1.0	27	3.88	0.45	441

Table 2
Gross kerogen components in TOC units, oil and gas potentials and intermediate results assessed from the suggested method over three different Upper Jurassic sections from the Danish Central Graben

Parameter	Bo-1, "Hot Unit"		Jeppe-1, "Hot Unit"		Jeppe-1, "Volg-20"	
TOC(observed) %wt	4.6		3.3		5.7	
S_2(observed) mg HC/g org.C	13.8		16.8		5.2	
Tr	0.0		0.3		0.4	
S_2(restored) mg HC/g org.C			24.0		8.7	
GORP	0.2		0		0.9	
TOC(restored) %wt	4.6		3.9		6.0	
TOC II	2.4 (3.0) %wt	52(66)%	3.5 (3.7) %wt	90 (95)%	0.3 (0.3) %wt	5%
TOC III	0.6 (0.8) %wt	14(17)%	0 %wt	0%	2.7 (3.2) %wt	45 (53)%
TOC IV	1.6 (0.8) %wt	34(17)%	0.4(0.2) %wt	10 (5)%	3.0 (2.5) %wt	50 (42)%
S_2 II(oil) mg HC/g org.C	11 (17.3)		24.0 (26.5)		0.9 (1.4)	
S_2 III(gas) mg HC/g org.C	2.8 (4.3)				7.8(13.1)	

Percentages in the TOC(oil), TOC(gas) and TOC(inert) columns indicate the average relative distributions of these components. Values corrected with respect to matrix effects, using Fig. 3 as a "worst" case, are shown in brackets.

carried out for the Bo-1 well assessing the carbon residue at 2.5 mg HC/g org.C reduces the TOC(inert) part to only 5%wt and increases the TOC(oil) from 90% to 95% (Table 2).

If the oil-prone end-member in this rich and good quality source rock section were increased to that of an Organic Facies AB, 800 mg HC/g org.C the oil-prone part would decrease to 71% and gas-prone will be 17% when no corrections have been made for matrix effects.

The Volgian section from Jeppe-1 (Table 1) is certainly more gas-prone. It is also localised stratigraphically in a more gas-prone and terrestrially influenced position (Damtoft et al., 1992). The hydrogen index values are generally very low, but some of the upper samples have reasonable hydrocarbon potentials although the section is now well into the oil window. The plot (Fig. 7) forms a reasonable trend, but with steeper inclination than the "Hot Unit" sections and with a high inertinite content (TOC(inert) = 3.0%wt,) suggested from the TOC axis intersection. The overlay for transformation ratio = 0.4 (Figs. 4(c) and 7) suggests the presence of a dominantly gas-prone section, (GORP = 0.9), but with some minor liquid potential (1-GORP = 0.1). The method suggests (Table 2) that the average composition of an immature equivalent of this section is 0.4, 2.1 and 3.0%wt for TOC(oil), TOC(gas) and TOC(inert), respectively. It further suggests that the dominantly gas-prone material has an average potential of 7.8 mg HC/g rock, whilst the liquid potential is 0.9 mg HC/g rock.

Considering a possible matrix retention effect of the size suggested by Fig. 3, increases the TOC(gas) to 3.2%wt and reduces the TOC(inert) to 2.5%wt. The oil-prone part is the same.

4.2. Comparison with other methods

In order to test and compare the S_2–TOC cross-plot method with other methods that splits the source kerogen into oil and gas potentials, samples from Upper Jurassic sections of Kimmerige Clay Fm. equivalents in four different North Sea wells have been analysed by Rock-Eval pyrolysis, combined pyrolysis and GC and quantitative marceral analysis. The shown sections are from two wells located in Norwegian Central Graben (Well 2/8-14) and the Northern Viking Graben (Well 30/9-10). The results (Table 3) are compiled in Figures 8 and 9 showing the GORP as vertical lines, representing the average gas-oil ratio derived from the presented cross-plot method. The discrete points are results from the other methods described above. Recontructed HI values have been used to derive the $G0$ from Pepper and Corvi's (1995) global curve. The fraction of vitrinite versus vitrinite plus liptinite gives the factor GM whilst the gas-oil-ratio factor G are derived from pyrolysis GC (area of C_1–C_5 versus C_{6+}).

Table 3
Rock-Eval, Pyrolysis GC, Gas index (*G*0) and marceral analysis used to compare methods that split source rock sections into oil and gas in Wells 2/8-14 and 30/9-10, Figs. 8 and 9

Depth	S_1	S_2	TOC	T_{max}	*G*0	HI	G	FFM+Lip. (%)	Vitrinite (%)	Inertinite (%)
Well 2/8-14										
3111.00								28.0	14.0	58.0
3186	3.01	9.00	2.88	424	0.23	312	0.19			
3189	1.51	6.00	2.19	424	0.25	274	0.21			
3192	0.59	1.46	0.98	428	0.30	149				
3195	1.91	9.07	2.50	423	0.22	363				
3198	2.18	10.22	2.88	430	0.22	355				
3207	4.31	27.10	6.37	422	0.20	425	0.26			
3210	5.76	36.31	8.64	424	0.21	420				
3213	6.16	35.54	8.38	423	0.20	424	0.26			
3216	6.16	37.75	8.68	424	0.20	435				
3219	5.47	34.70	8.24	426	0.21	421	0.29			
3222	4.25	25.80	6.56	424	0.21	393				
3225	5.08	34.96	8.17	422	0.20	428	0.29			
3228	4.28	29.53	7.06	425	0.21	418				
3231	5.06	37.56	8.18	428	0.20	459				
3234	5.04	32.17	7.07	428	0.20	455	0.24			
3237	4.26	28.51	6.43	429	0.20	443				
3240	5.21	34.98	8.04	425	0.20	435				
3243	3.92	29.45	6.62	427	0.20	445	0.21			
3246	1.28	8.84	2.53	432	0.22	349				
3249	0.88	34.76	3.45	394	0.11	1008				
3276	3.20	21.97	5.35	426	0.21	411				
3285	2.09	15.40	4.37	426	0.22	352	0.45	67.0	3.0	30.0
3294	3.33	24.14	6.26	429	0.21	386				
3300	3.90	31.34	7.28	426	0.20	430				
3303	1.86	15.69	4.13	427	0.22	380				
3306	1.92	14.24	3.96	425	0.22	360		71.0	4.0	25.0
3381	0.74	5.89	2.33	429	0.26	253				
3414	3.90	33.38	7.55	434	0.20	442		75.0	4.0	21.0
3417	4.12	33.84	7.64	432	0.20	443				
3420	3.32	25.75	6.28	435	0.21	410				
3423	3.39	26.11	6.87	431	0.22	380				
3426	3.10	24.69	6.19	432	0.21	399	0.27			
3429	3.33	25.90	6.18	430	0.21	419				
3438	4.11	33.29	8.41	435	0.21	396				
3441	4.32	39.03	8.36	431	0.20	467				
3462	3.98	36.26	9.36	435	0.22	387				
3480	2.70	20.53	5.40	438	0.22	380				
3519	1.16	3.68	1.76	427	0.27	209		85.0	4.0	11.0
3540	3.16	21.77	6.10	440	0.22	357				
3570	0.55	3.95	1.96	435	0.27	202				
3576	0.82	3.11	1.38	433	0.27	225		83.0	3.0	14.0
3690	0.99	5.46	3.15	436	0.29	173				
3693	2.06	12.61	4.66	437	0.25	271				
3699	2.11	16.74	9.17	434	0.28	183				
3711	1.47	10.52	4.88	436	0.26	216		81.0	6.0	13.0
3720	2.03	13.49	5.03	439	0.25	268				
3729	1.91	12.34	4.53	438	0.25	272				
3756	1.86	10.75	7.37	436	0.30	146				
3900	1.15	4.49	3.36	437	0.31	134		86.0	3.0	11.0
4002	0.43	3.65	5.44	432	0.36	67				
4080	1.22	5.52	2.88	442	0.28	192				
4119	0.78	4.08	2.70	441	0.30	151		93.0	3.0	4.0
4182	0.73	2.93	2.10	441	0.30	140				
4200	0.93	3.72	2.34	443	0.30	159		55.0	6.0	39.0

Table 3 (*continued*)

Depth	S_1	S_2	TOC	T_{max}	*G*0	HI	G	FFM+Lip. (%)	Vitrinite (%)	Inertinite (%)
4302	1.04	2.59	2.28	438	0.32	114		63.0	4.0	33.0
4362	2.70	3.40	2.65	434	0.31	128				
4380	0.91	1.90	1.40	438	0.31	136				
Well 30/9-10										
1570					0.00			45.8	0.0	54.2
2720.00	0.42	12.18	3.54	427	0.22	344				
2722.00	0.68	16.09	4.35	425	0.22	370		69.0	9.0	22.0
2725.10	1.16	19.42	4.86	428	0.21	400	0.26			
2727.00					0.00		0.31			
2730.40	0.99	17.11	4.61	427	0.22	371		68.0	3.5	28.5
2731.16					0.00		0.19			
2747.00	2.41	24.47	6.62	418	0.22	370	0.23			
2754.90	0.75	2.94	3.57	419	0.00	82	0.4			
2759.17	3.15	35.51	10.29	424	0.22	345		75.0	6.0	19.0
2760.43					0.00		0.25			
2764.14	3.85	63.69	13.71	422	0.20	465				
2767.00	1.93	6.92	2.76	418	0.00	251				
2771.96	2.37	28.37	7.20	420	0.21	394	0.26	66.7	3.6	29.7
2774.90	1.01	15.36	4.64	422	0.00	331	0.27			
2778.75					0.00		0.28			
2780.00	1.77	30.26	7.14	422	0.21	424				
2782.00	1.66	32.18	7.11	419	0.20	453	0.27			
2785.00	0.81	10.12	2.47	422	0.21	410		77.0	5.0	18.0
2885.00	0.75	8.79	8.12	428	0.32	108		23.0	28.0	49.0
2985.00	0.60	11.44	7.94	425	0.31	144		18.0	31.0	51.0
3085.00	2.29	40.25	23.67	433	0.30	170				
3185.00	0.16	1.45	1.48	434	0.34	98				
3285.00	1.27	10.06	2.49	434	0.21	404				
3385.00	0.26	1.85	1.33	435	0.31	139				
3485.00	0.39	1.83	1.31	440	0.31	140				
3585.00	0.18	0.47	0.57	444	0.35	82				
3642.00	0.35	2.30	1.48	427	0.30	155				

In Well 2/8-14(Fig. 8) the *G* and *G*0 are quite close to the GORP line, suggesting a dominantly oil-prone source rock section with gas ratio close to 0.2. The *G* data are, however, consistently larger (more gas-prone) than both the GORP and *G*0 data. The marceral results (GM) are significantly lower (more oil-prone) than the results from the other methods.

In Well 30/9-10 (Fig. 9) the *G* and *G*0 results are again close to the GORP vertical line showing a gas ratio slightly above 0.2, again a section with a significant oil potential. The few marceral results from this section are again significantly lower then the other gas-oil-ratio parameters. The results from the other wells in the study show similar results with the marcerals giving very low gas ratios.

The *G*0 factor seems to follow the GORP and pyrolysis GC results in all these source rock sections. Deviation between the *G*0 and GORP is, however, expected in more gas-prone sections because the *G*0 never exceeds 0.6 (Pepper and Corvi, 1995). The GORP will extend over the whole range from 0 to 1.0. It is necessary to analyse and compare more gas-prone sections in order to verify this postulated discrepancy.

4.3. Can S_2–TOC plots give sedimentolgical information?

During many projects using this method certain patterns seem to occur. There are many examples where one section falls on a fairly straight line whilst the section or formation above or below shifts to another consistent trend. In other situations shifts may occur between smooth trends and chaotic patterns.

The plot in Fig. 10 is made from results taken from the paper by Robison and Engel (1993) who analysed a transgressive organic rich section of Late Cretaceous age in Egypt. They had subdivided the section into sequence stratigraphic units of transgressive (T) and high stand (H) system tracts. The plot (Fig. 10) shows very clearly how the transgressive system tracts form smooth low angle (larger amount of oil-prone organic carbon) close to linear trends, whilst the high stand system tracts change towards a steeper angle (more gas-prone material)

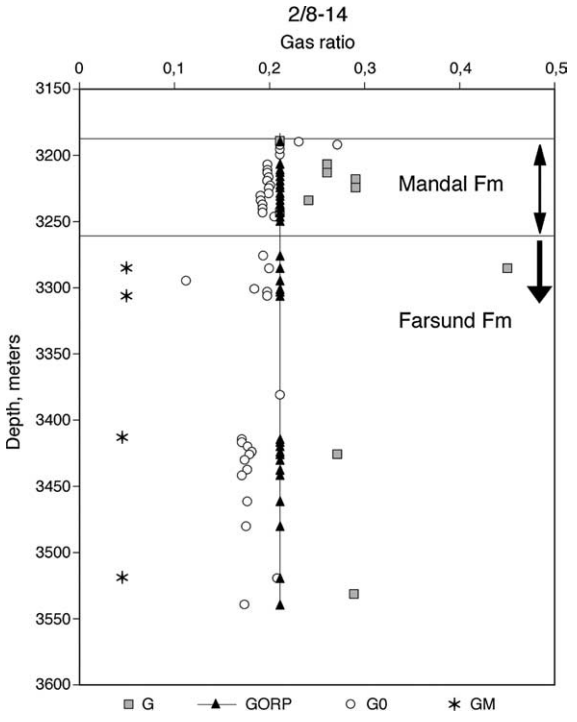

Fig. 8. Comparison of results from methods used to split the total potential into oil and gas potentials in the Upper Jurassic source rock section of Well 2/8-14. See text for further explanations.

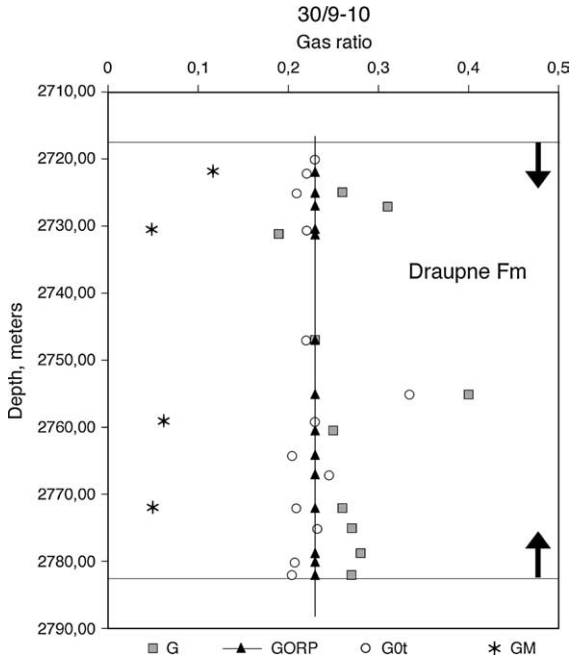

Fig. 9. Comparison of results from various geochemical methods used to split the total potential into oil and gas potentials in the Upper Jurassic source rock section of Well 30/9-10. See text for further explanations.

with a more chaotic pattern. The transgressive system tracts occur when the sea level is rising and the basin becomes more and more flooded with less influx from terrestrial and reworked (inert) organic material. During the high stand system tract the sea level drops and more and more terrestrially derived and reworked organic

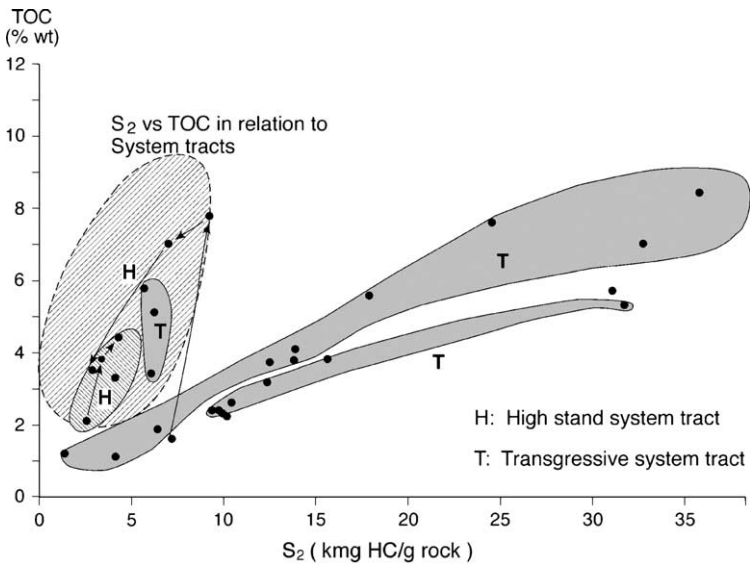

Fig. 10. Plot of S_2 versus TOC from alternating high stand and transgressive system tracts of Late Creataceous shales from Egypt (Robison and Engel, 1993).

Table 4
A constructed sedimetological cycle with transgressive and high stand system tract and resulting S_2 and TOC values from selected oil- and gas-prone TOC with HI end-members

System tract	TOC (oil) (%wt)	TOC(gas) (%wt)	TOC (inertinite) (%wt)	HI II (mg HC/g org.C)	HI III (mg HC/g org.C)	S_2 (mg HC/g rock)	TOC (% wt)
T, transgressive	1	1	1	700	250	9.5	3
T, transgressive	2	1	2	700	250	16.5	5
T, transgressive	3	1	3	700	250	23.5	7
T, transgressive	2	2	2	700	250	19	6
H, high stand	0.8	2	2	700	250	10.6	4.8
H, high stand	0.2	2.5	3	700	250	7.65	5.70
H, high stand	0.2	3	3	700	250	8.9	6.2
H, high stand	0.2	3	4	700	250	8.9	7.2
H, high stand	1.0	2	3	700	250	12	6
H, high stand	1.0	3	3	700	250	14.5	7
T, transgressive	2.5	3	2	700	250	25	7.5
T, transgressive	3	3	1	700	250	28.5	7
T, transgressive	4	3	2	700	250	35.5	9
T, transgressive	5	3	3	700	250	42.5	11
T, transgressive	4	4	2	700	250	38	10

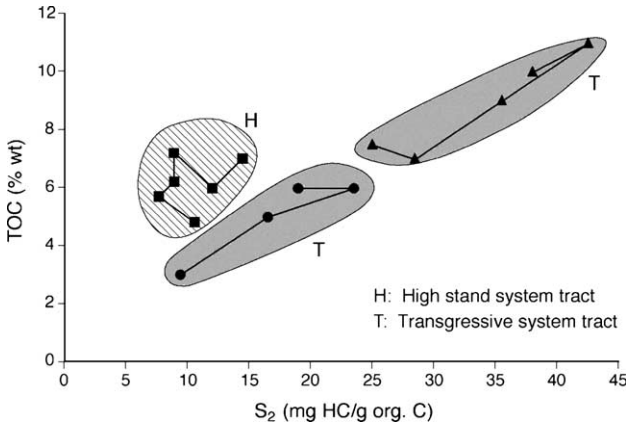

Fig. 11. S_2 versus TOC plot from a constructed (Table 4) alternating high stand and transgressive system tracts using TOC constituents with associated HI end-members.

material (with lower HI values) are coming into the basin. This is one case where the pattern in a S_2–TOC plot can be explained by the sedimentology of the section.

It also leads the suggestion that an end-member model could be set up together with a sedimentological model in order to predict source rock oil and gas potential by using the algorithm:

$$\mathrm{TOC} = \mathrm{TOC(oil)} + \mathrm{TOC(gas)} + \mathrm{TOC(inert)} \quad (19)$$

and

$$S_2 = \mathrm{TOC(oil)} * \mathrm{HI(oil)} + \mathrm{TOC(gas)} * \mathrm{HI(gas)} + \mathrm{TOC(inert)}. \quad (20)$$

S_2–TOC plot could be used as a calibration or checking tool for such models. A constructed example is set up in Table 4 and Fig. 11 where the terrestrial componets, TOC (gas) and TOC (inert), in the high stand period (H) are similar to the transgressive periods (T) whilst the aquatic componet, TOC (oil) is lowered. It is not an attempt to mimic the results in Fig. 10, but rather a simple example that shows the expression of the system tracts in the S_2–TOC plot. This model leads to fairly linear transgressive S_2–TOC trends and a more chaotic, non-linear high stand system trend.

5. Conclusions

A method has been developed to assess average gross kerogen types in source rock horizons. The method is based upon Rock-Eval potential (S_2) and TOC values,

information that is very common in geochemical databases. It is based upon the assumption that kerogen end-members with assigned HI values exist. From suggested algorithms, the average amounts of oil-prone, gas-prone and "dead" kerogen can be determined as TOC(oil), TOC(gas) and TOC(inert) over source rock intervals. These values can be transformed into source rock potentials for oil and gas producing constituents via the hydrogen indices of the ideal kerogen end-members.

For practical application of the method, we suggest that a set of "quick-look" overlays for various transformation stages be used. The overlays will enable the user to easily assess the relative compositions of *oil*- and *gas*-prone kerogens when the data from the analysed section are plotted on a standard scale format.

Results from the presented method can be influenced by matrix-induced errors in Rock-Eval pyrolysis. This effect, which occurs for oil-prone kerogens and adsorptive minerals, can cause problems for lean samples (S_2 = 0–3 mg HC/g rock), and such low values may be multiplied by a factor close to 3 in order to obtain the real S_2 value. Results in the range S_2 = 3–25 mg HC/g rock need to be corrected with respect to the TOC (inert), and rich samples (up to 60 mg HC/g rock) need a minor progressively decreasing correction factor plus corrections with respect to the TOC (inert).

Experience using the method suggests that sedimentological, system tract information may be derived from S_2–TOC cross-plots. A constructed modelling example suggests that the end-member concept used in this approach may be used in forward type source rock prediction models when combined with sedimentological models.

Acknowledgements

The authors thank the Norwegian Research Council (project NFR 480.95/008) and the oil companies Amoco Norway Oil, Co and Mobil Exploration Norway for financial support. We are also grateful to Drs. Alton Brown and David K. Baskin for helpful comments and suggestions that improved this paper.

Guest Associate Editor—**Mark A. McCaffrey**

References

Andsbjerg, J., Dybkjaer, K., 2003. Sequence startigraphy of the Jurassic of the Danish Central Graben. In: Ineson, J.R., Surlyk, F. (Eds.), The Jurassic of Deenmark and Greenland. The Geological Survey of Denmark and Greenland Bulletin 1, 265–300.

Barnard, P.C., Collins, A.G., Cooper, B.S., 1981. Identification and distribution of kerogen facies in a source rock horizon-examples from the North Sea Basin. In: Brooks, J. (Ed.), Organic Maturation Studies and Fossil Fuel Exploration. Academic Press, London, pp. 271–282.

Baskin, D.K., 1997. Atomic H/C ratio of kerogen as an estimate of thermal maturity and organic matter conversion. American Association of Petroleum Geologists Bulletin 81, 1437–1450.

Clayton, J.L., Ryder, R.T., 1984. Organic geochemistry of black shales and oils in the Minnelusa Formation (Permian and Pennsylvanian), Powder River basin, Wyoming. In: Woodward, J., Meissner, F.F., Clayton, J.L. (Eds.), Hydrocarbon Source Rocks of the Greater Rocky Mountain Region. Rocky Mt. Assoc. Geol., Denver, CO, pp. 231–253.

Cooles, G.P., MacKenzie, A.S., Quigley, T.M., 1986. Calculation of petroleum masses generated and expelled from source rocks. Organic Geochemistry 10, 235–245.

Cooper, B.S., Barnard, P.C., 1984. Source rocks and oils of the central and northern North Sea. In: Demaison, G., Murris, R.J. (Eds.), Petroleum Geochemistry and Basin Evaluation, AAPG Memoir 35. American Association of Petroleum Geologists, Tulsa, pp. 1–14.

Cornford, C., 1994. The Mandal-Ekofisk(!) Petroleum System in the Central Graben of the North Sea. In: Magoon, L.B., Dow, W.G. (Eds.), From Source to Trap. AAPG Memoir 60. American Association of Petroleum Geologists, Tulsa, pp. 537–571.

Cornford, C., Gardner, P., Burgess, C., 1998. Geochemical truths in large data sets I: Geochemical screening data. Organic Geochemistry 29, 519–530.

Dahl, B., Augustson, J.H., 1993. The influence of Tertiary and Quaternary sedimentation and erosion on the hydrocarbon generation in Norwegian offshore basins. In: Dore, A.G. et al. (Eds.), Basin Modelling: Advances and Applications, Norwegian Petroleum Scociety (NPF), Special Publication 3. Elsevier, Amsterdam, pp. 419–431.

Dahl, B., Meisingset, I., 1996. Prospect resource assessment using an integrated system of basin simulation and geological mapping software: examples from the North Sea. In: Doré, A.G., Sinding-Larsen, R. (Eds.), Quantification and Prediction of Petroleum Resources, Norwegian Petroleum Society (NPF), Special Publication 6. Elsevier, Amsterdam, pp. 237–251.

Dahl, B., Yukler, M.A., 1991. The role of petroleum geochemistry in basin modelling of the Oseberg Area, North Sea. In: Merrill, R.K. (Ed.), AAPG Treatise of Petroleum Geology Handbook. Source and Migration Processes and Evaluation Techniques. American Association of Petroleum Geologists, Tulsa, pp. 65–85.

Damtoft, K., Nielsen, L.H., Johannessen, P.N., Thomsen, E., Andersen, P.R., 1992. Hydrocarbon plays of the Danish Central Trough. In: Spencer, A.M. (Ed.), Generation, Accumulation and Production of Europe's Hydrocarbons II, Special Publication of the European Association of Petroleum Geoscientists No. 2. Springer, Berlin, pp. 35–58.

Demaison, G.J., Moore, G.T., 1980. Anoxic environments and oil source bed genesis. American Association of Petroleum Geologists Bulletin 64 (8), 1179–1209.

Espitalié, J., Bordenave, M.L., 1993. Rock-Eval pyrolysis. In: Bordenave, M.L. (Ed.), Applied Petroleum Geochemistry. Editions Technip, Paris, pp. 237–261.

Espitalié, J., Marquis, F., Sage, L., 1987. Organic geochemistry of the Paris Basin. In: Brooks, J., Glennie, K. (Eds.), Petroleum Geology of North West Europe. Graham & Trotman, pp. 71–86.

Espitalié, J., Madec, M., Tissot, B., 1980. Role of mineral matrix in kerogen pyrolysis: influence on petroleum generation and migration. American Association of Petroleum Geologists Bulletin 4 (1), 59–66.

Horsfield, B., 1989. Practical criteria for classifying kerogens: some observations from pyrolysis-gas chromatography. Geochimica et Cosmochimica 53, 891–901.

Hunt, J.M., 1996. Petroleum Geochemistry and Geology, second ed. Freeman, New York.

Isaksen, G.H., Ledje, H., 2001. Source rock quality and hydrocarbon migration patways within the Greater Utsira High Area, Viking Graben, Norwegian North Sea. American Association of Petroleum Geologists Bulletin 85 (5), 861–883.

Jones, R.W., 1987. Organic facies. In: Brooks, J., Welte, D.H. (Eds.), Advances in Petroleum Geochemistry. Academic Press, New York, pp. 1–90.

Jones, R.W., Edison, A., 1978. Microscopic observations of kerogen related to geochemical parameters with emphasise on thermal maturation. In: Oltz, D.F. (Ed.), Low Temperature Metamorphism of Kerogen and Clay Minerals. SEPM, Pacific section, pp. 1–12.

Justwan, H., Dahl, B., 2005. Quantitative hydrocarbon potential mapping and organofacies study in the greater Balder Area, Norwegian North Sea. In: Doré, A.G., Vining, B. (Eds.), Petroleum Geology: North West Europe and Global Perspectives – Proceedings of the 6th Petroleum Geology Conference, in press.

Katz, B.J., 1983. Limitations of Rock-Eval pyrolysis for typing of organic matter. Organic Geochemistry 4, 195–199.

Langford, F.F., Blanc-Valleron, M.-M., 1990. Interpreting Rock-Eval pyrolysis data using graphs of pyrolizable hydrocarbons vs. total organic carbon. American Association of Petroleum Geologists Bulletin 74 (6), 799–804.

Mukhopadhyay, P.K., Hagemann, H.W., Gormly, J.R., 1985. Characterization of kerogens as seen under the aspect of maturation and hydrocarbon generation. Erdö u. Kohle – Edgas – Petrochem. V. mit Brennstoff-Chem. 38, 7–18.

Pepper, A.S., Corvi, P.J., 1995. Simple kinetic models of petroleum formation. Part I: oil and gas generation from kerogen. Marine Petroleum Geology 12 (3), 291–319.

Peters, K.E., 1986. Guidelines for evaluating petroleum source rock using programmed pyrolysis. American Association of Petroleum Geologists Bulletin 70 (3), 318–329.

Robison, V.D., Engel, M.H., 1993. Characterisation of the source horizons within the late cretaceous transgressive sequence of Egypt. In: Katz, B.J., Pratt, L.M. (Eds.), Source Rocks in a Stratigraphic Framework. AAPG Studies in Geology #37, pp. 101–117.

Thomas, B.M., Møller Pedersen, P., Whitaker, M.F., Shaw, N.D., 1985. Organic facies and hydrocarbon distributions in the Norwegian North Sea. In: Thomas, B.M. (Ed.), Petroleum Geochemistry, Exploration of the Norwegian Shelf. Norwegian Petroleum Society (Graham & Trotman), London, pp. 3–26.

Tissot, B.P., Welte, D.H., 1978. Petroleum Formation and Occurrence. Springer, Berlin.

Tyson, R.V., 1995. Sedimentary Organic Matter. Organic Facies and Palynofacies. Chapman & Hall, London.